

# SiC's Potential Impact on the Design of Wind Generation System

Hui Zhang<sup>1</sup>, Leon M. Tolbert<sup>1,2</sup>  
 hzhang18@utk.edu, tolbert@utk.edu

<sup>1</sup>Electrical Engineering and Computer Science  
 The University of Tennessee  
 Knoxville, TN 37996-2100

<sup>2</sup>Power Electronics & Electric Machinery Research Center  
 Oak Ridge National Laboratory  
 Knoxville, TN 37932

**Abstract** — The potential impact of SiC devices on a wind generation system is explored by simulations in this work. The system modeling is explained in detail. Most recent SiC MOSFET prototypes are obtained, tested, and used to form a bi-directional converter in the simulation. The performance of the SiC converter is analyzed and compared to its Si counterpart at different temperatures and frequencies. A conclusion is drawn that the SiC converters can improve the wind system efficiency, conserve energy, and reduce system size and cost due to the low-loss, high-frequency, and high-temperature properties of SiC devices even for one-for-one replacement for Si devices.

**Keywords** — Silicon carbide (SiC), MOSFET, converter, wind generation, modeling.

## I. INTRODUCTION

The underlying premise of the application is that SiC devices would reduce substantially the cost of energy of large wind turbines that use power electronics to allow for variable speed generation. Variable speed capability allows the wind turbine to operate at the speeds which produce the greatest amount of power and minimizes torque perturbations in the drive train. This capability tends to decrease the overall cost of energy because the amount of energy generated is increased, and the cost of the drive train and its maintenance are reduced. Since the voltage and frequency of the generated power vary with turbine speed, a converter is required to reconcile the output with the fixed voltage and frequency of the grid. SiC-based power devices have several advantages, including lower losses, higher temperature, and faster switching. These can be exploited to reduce losses and increase net energy production. The lower losses, along with higher temperature, can be exploited to improve the reliability of the converter, thus potentially reduce the cost of the converter.

One of the key purposes of this work is to simulate the

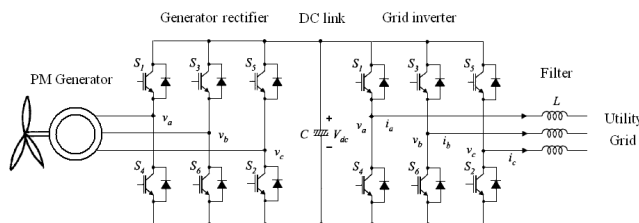


Fig. 1. Wind generation system structure.

performance of SiC-based converters that might be used in a wind turbine, and compare to the commonly used Si converters.

## II. SYSTEM MODELING

A wind generation system is designed based on a National Renewable Energy Laboratory (NREL) baseline wind turbine described by [1]. It is composed of a 1.5MW wind turbine, a permanent magnet (PM) generator rated at 690 V, a bi-directional converter comprised of two back-to-back inverters, and a utility filter (simplified as a single inductance), as shown as Fig. 1 [2]. The wind energy is converted to electricity by the PM generator, and then transferred to the utility. In this process, the back-to-back converter plays two roles, one is to control the generator to catch as much wind energy as possible (high switching speed is desirable), and the other is to deliver the energy to the utility. In both roles, the power loss in the converter is of the most concern, which not only determines the design of the converter but also affects other components in the system, such as the filter. This will be analyzed using simulation method in this work, and the associated modeling work is presented in the following paragraphs.

### A. PM Generator

The input power  $P_{in}$  (kW) and the speed of the generator  $n_g$  (rpm) at a certain wind speed are given as the inputs of the simulation system. The electrical parameters of the generator, are given in Table I. Assume the generator back Emf is in phase with the generator current, then parameters for the generator rectifier can be solved in  $dq$  rotating coordinate system based on basic PM generator theory as follows:

Generator frequency,  $f_g$  (subscript '0' denotes the parameter's value at rated speed  $n_0$ ):

$$f_g = \frac{p \cdot n}{120} \quad f_{g0} = \frac{p \cdot n_0}{120} \quad (1)$$

Back Emf (line-neutral, peak),  $Emf$

$$Emf = Emf_0 \cdot \frac{f_g}{f_{g0}} \quad (2)$$

Core losses,  $P_{lc}$ , eddy loss,  $P_{le}$ , and hysteresis loss,  $P_{lh}$ :

$$P_{lc} = P_{le} + P_{lh} \quad P_{le} = P_{le0} \cdot \frac{f_g}{f_{g0}} \quad P_{lh} = P_{lh0} \cdot \frac{f_g}{f_{g0}} \quad (3)$$

TABLE I. WIND GENERATION SYSTEM PARAMETERS

Generator parameters	
Rated power, MW	1.5
Nominal voltage, V	690
Rated speed $n_0$ , rpm	164
Back Emf at $n_0$ , $Emf_0$ , V	150
Base machine pole number $p$	56
Stator phase resistance $R$ , $\Omega$	1.23e-2
Stator phase inductance $L$ , H	6.62e-4
Eddy loss at $n_0$ , $P_{le0}$ , kW	4.284
Hysteresis loss at $n_0$ , $P_{h0}$ , kW	1.848
Others	
DC link voltage $V_{dc}$ , V	1100
Grid voltage $V_{ll}$ , V	690
Grid power factor, $\cos\phi$	0.95
filter loss constant, $k$	0.0097

Phase current on  $q$ -axis (peak),  $I_{sq}$ :

$$I_{sq} = \frac{1000 \cdot P_m \cdot 2}{3 \cdot Emf} \quad (4)$$

Output voltage without considering the core losses,  $E_c$ :

$$E_c = \sqrt{(Emf - I_{sq}R)^2 + (I_{sq}X)^2} \quad X = \omega_g L \quad \omega_g = 2\pi f_g \quad (5)$$

Effective current due to core losses (peak),  $I_c$ ,  $I_{cq}$  ( $q$ -axis component),  $I_{cd}$  ( $d$ -axis component):

$$I_c = \frac{1000 \cdot P_{lc} \cdot 2}{3 \cdot E_c}$$

$$I_{cq} = I_c \cdot \cos\phi_c \quad I_{cd} = I_c \cdot \sin\phi_c \quad \phi_c = \arccos\left(\frac{E_c}{Emf}\right) \quad (6)$$

Total phase current (peak),  $I_s$ :

$$I_s = \sqrt{I_{stq}^2 + I_{std}^2} \\ I_{stq} = I_{sq} + I_{cq} \quad I_{std} = I_{sd} + I_{cd} \quad (7)$$

Output voltage (peak),  $U_{gout}$ :

$$U_{gout} = \sqrt{U_{sq}^2 + U_{sd}^2} \\ U_{sq} = Emf - I_{std}X - I_{stq}R \quad U_{sd} = I_{stq}X - I_{std}R \quad (8)$$

Power factor,  $\cos\phi$ :

$$\cos\phi = \cos(\alpha_I - \alpha_U) \\ \alpha_I = \arctan\left(\frac{I_{stq}}{I_{std}}\right) \quad \alpha_U = \arctan\left(\frac{U_{sq}}{U_{sd}}\right) \quad (9)$$

Copper loss,  $P_{lcu}$ :

$$P_{lcu} = \frac{3 \cdot I_s^2 \cdot R}{2 \cdot 1000} \quad (10)$$

Generator efficiency,  $\eta_g$ :

$$\eta_g = \frac{P_{in} - P_{lcu} - P_{lc}}{P_{in}} \times 100\% \quad (11)$$

Rectifier modulation index,  $M_r$ :

$$M_r = \frac{U_{gout}}{V_{dc}/2} \quad (12)$$

For the grid inverter, if the power loss of the DC link capacitor is neglected, the input power of the grid inverter is equal to the output power of the generator rectifier. Then, for a certain grid output voltage  $V_{ll}$  (line-line, rms) and power factor  $\cos\phi$ , the phase current (peak)  $I_{grid}$  is

$$I_{grid} = \frac{\sqrt{2}P_{in}\eta}{\sqrt{3}V_{ll}\cos\phi}, \quad (13)$$

and its modulation index  $M_i$  is

$$M_i = \frac{2\sqrt{2}\cdot V_{ll}}{\sqrt{3}\cdot V_{dc}}. \quad (14)$$

Also, the filter loss  $P_{fj}$  is considered when calculating the system efficiency.

$$P_{fj} = k \cdot I_{grid}^2, \quad (15)$$

where  $k$  is filter loss constant.

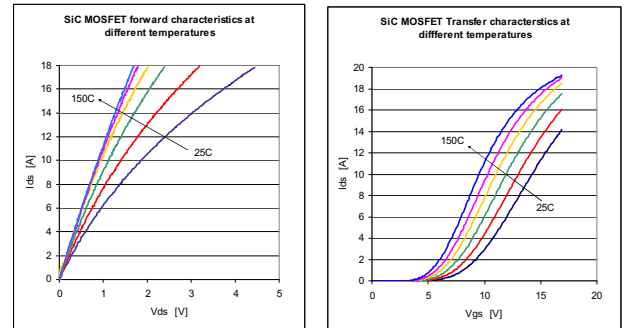
## B. Converter

A 1.5MW converter is required to provide full power conditioning for the full output of the generator. Because no SiC devices are presently available at this rating, the converter is assumed to be composed of 10 SiC-based converters rated at 150 kW in the simulation, which are based on the devices listed in Table II. The multiples in voltage column mean the number of devices in series, and that in current column mean the number of devices in parallel.

The SiC MOSFET prototypes are tested for both static and dynamic characteristics. As shown in Fig. 2, the on-state resistance of the SiC MOSFET decreases with temperature from 25 °C to 150 °C, and thus the conduction loss decreases with temperature. Newer SiC MOSFETs from CREE exhibit

TABLE II. DEVICES USED IN THE CONVERTERS

Item	Voltage rating	Current rating	Part number
SiC MOSFETs	800V×2	10A×20	CREE, Prototype
SiC Schottky diodes	1200V	10A×20	CREE, C2D10120
Si IGBT Modules	1700V	200	DYNEX, DIM200WHS17



(a) Forward characteristics

(b) Transfer characteristics

Fig. 2. Static characteristics of the SiC MOSFET at different temperatures.

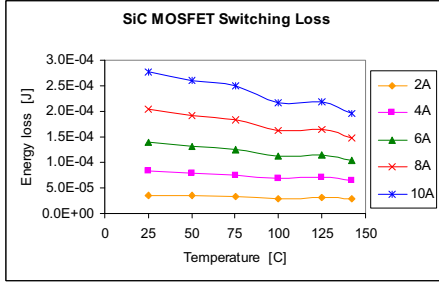


Fig. 3. Switching losses of the SiC MOSFET at different temperatures.

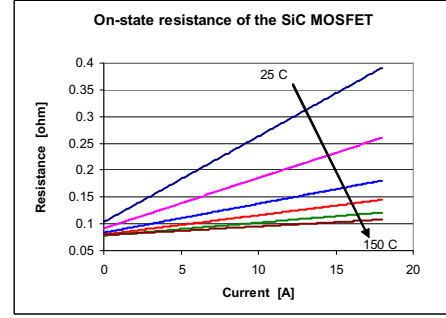


Fig. 4. On-state resistance of the SiC MOSFET.

different dependency of on-state resistance with temperature; the on-state resistance in the newer SiC MOSFETs begins to increase at around 100 °C. The switching energy losses of the tested devices at different temperatures and different current levels are shown in Fig. 3. It indicates that the switching loss decreases with temperature and increases with current.

### C. Power Loss Models

A widely used averaging technique [3-6] is employed to study the inverter power loss. This technique gets a sample in each switching cycle, and then uses these values to find the effective value at the fundamental cycle of the output. The resultant equations are presented in the following paragraphs. For more details, please see [7] [8].

For SiC MOSFETs, the conduction loss is mainly caused by on-state resistance,  $R_{on}$ . It is calculated by

$$P_{cond, M} = I^2 R_{on} \left( \frac{1}{8} + \frac{1}{3\pi} M \cos \phi \right), \quad (16)$$

where  $M$  is modulation index,  $I$  is the peak of phase current, and  $\phi$  is phase angle. For SiC Schottky diode and Si IGBT, the voltage drop is not zero when current is zero. So there is additional loss associate to this voltage drop,  $V_0$ . Conductive loss equations are shown as (17) for the diode and (18) for the IGBT.

$$P_{D, cond} = I^2 \cdot R_{on} \left( \frac{1}{8} - \frac{1}{3\pi} M \cos \phi \right) + I \cdot V_0 \cdot \left( \frac{1}{2\pi} - \frac{M \cos \phi}{8} \right) \quad (17)$$

$$P_{I, cond} = I^2 \cdot R_{on} \left( \frac{1}{8} + \frac{1}{3\pi} M \cos \phi \right) + I \cdot V_0 \cdot \left( \frac{1}{2\pi} + \frac{M \cos \phi}{8} \right) \quad (18)$$

The value of  $R_{on}$  changes with the current and temperature. Look-up tables are used to find correct value of  $R_{on}$  in the simulations. Fig. 4 shows the table for the SiC MOSFET based on the test data in Fig. 2. Similar tables can be made for diodes and IGBT, which are based on manufacturer values [9] [10].

As shown in Fig. 3, the switching energy loss of the SiC MOSFET is a function of current at a specific temperature. It can be expressed as a polynomial of current.

$$E(i) = ai^3 + bi^2 + ci + d, \quad (19)$$

where  $a$ ,  $b$ ,  $c$ ,  $d$  are coefficients which are obtained from the curve fitting of experimental data, and are different at different

temperatures. Then, the effective switching power loss for a SPWM controlled inverter is expressed as

$$P_{sw} = f_{sw} \cdot \left( \frac{2a}{3\pi} I^3 + \frac{b}{4} I^2 + \frac{c}{\pi} I + \frac{d}{2} \right). \quad (20)$$

The look-up table based on (20) is shown in Fig. 5. The same method can be applied to diodes and IGBT.

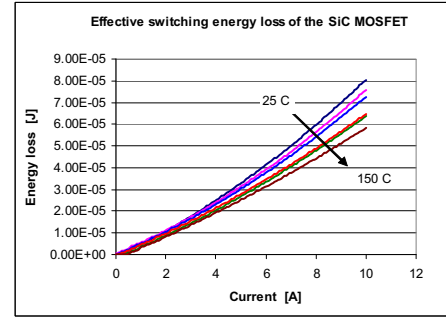


Fig. 5. Effective switching energy loss of the SiC MOSFET in an inverter.

### D. Thermal Models

The equivalent thermal circuit shown in Fig. 6 is used to analyze the thermal response of the converter [7] [8]. It can be solved in frequency domain. The transfer functions are shown below:

$$Z_{jic}(s) = \frac{R_{jj1}}{1 + s\tau_{jj1}} + \frac{R_{jj2}}{1 + s\tau_{jj2}} + \dots + \frac{R_{jcn}}{1 + s\tau_{jcn}}, \quad (21)$$

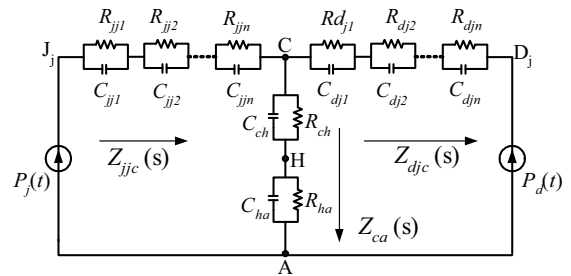


Fig. 6. Thermal equivalent circuit of an inverter.

$$Z_{dj c}(s) = \frac{R_{dj1}}{1+s\tau_{dj1}} + \frac{R_{dj2}}{1+s\tau_{dj2}} + \dots + \frac{R_{dj n}}{1+s\tau_{dj n}}, \quad (22)$$

$$Z_{ca}(s) = \frac{R_{ch}}{1+s\tau_{ch}} + \frac{R_{ha}}{1+s\tau_{ha}}. \quad (23)$$

In (21) – (23),  $R$  is the thermal resistance, and  $\tau$  is the thermal time constant. Manufacturer data is used in the simulations.

### III. SIMULATIONS AND DISCUSSIONS

The simulation of this wind generation system is done for the wind speed range from 6 m/s to 11 m/s, which has the best energy density. Different switching frequencies are also studied. In order to compare the SiC converter to the Si one, the junction temperature limit for both systems is assumed to be 150 °C.

#### A. At Switching Frequency of 3 kHz

Currently, most of commercial wind turbine converters are switched at 3 kHz. The generator is designed to work at rated power at the wind speed of 11 m/s, and at the above speeds, it keeps the rated speed and power. By the simulation, from 6m/s to 11 m/s, the converter efficiency (including two inverters and the power loss of the filter) is shown in Fig. 7. At the whole speed range, the efficiency of the Si converter is lower than that of the SiC converter. More specifically, the average efficiency of the SiC converter is 98.0 % compared to 94.6 % of the Si converter. The average power loss saved by the SiC converter is about 65.8 % of that of the Si converter. At the worst case (wind speed 11 m/s), it is about 50.8 kW.

The average power loss percentage of each component in the wind generation systems is shown in Fig. 8. The efficiencies of the generators in the two systems are the same (96.4 % on average) whether the Si or the SiC converter is used. However, for the Si-based system, the converter loss accounts for the most, which is as large as 47.7 % (compared to 18.8% of the SiC-based system). Thus, it is necessary to reduce the loss in the converter in order to improve the generation system efficiency. The SiC converter is a good alternative.

#### B. At Frequency up to 50 kHz

On the other hand, Fig. 8 demonstrates that the power loss

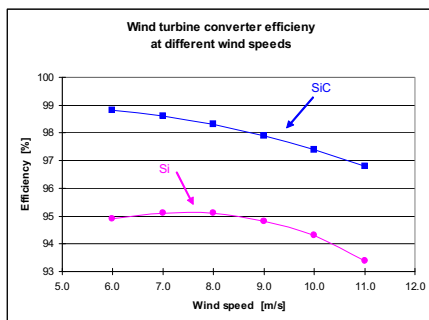


Fig. 7. Efficiency of SiC and Si based wind turbine converters at different wind speeds.

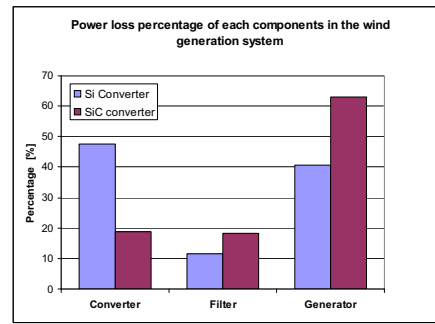


Fig. 8. Power loss breakdown in the wind generation system.

of the filter also accounts for a big portion for the both converters (11.6 % for Si vs. 18.3 % for SiC-based system). The size and loss of the filter is related to the switching frequency of the converter. Improving the switching frequency of the converter can reduce the size and loss of the filter, and thus the cost. Since high switching frequency is one of the merits of SiC devices, improving the switching frequency of the converter in this application might be considered.

As shown in Fig. 9, as frequency increases from 1 kHz to 50 kHz, the efficiency of the SiC converter (not including filter loss) at rated power and 150 °C is linearly decreased at a rate of 0.4 % per 5 kHz, and that of the Si converter decreases much more quickly at a rate of about 4.9 % per 5 kHz. In practice, the switching frequency of a large power electronic Si IGBT can not exceed 20 kHz because of the large amount of loss. For this case, the efficiency of the Si converter at 20 kHz is 76.6 %, which is not acceptable. While for the SiC converter, it has a relative high efficiency of 95.2 % even at 50 kHz. Thus, it is possible to improve efficiency and reduce the cost of the system at the same time by using the SiC converter. For example, increasing the switching frequency of the SiC converter to 21 kHz, its efficiency is 97.5 %, which obtains 2.2% advantage in efficiency compared to the Si converter switching at 3 kHz, and at the same time, the size, loss, and cost of the filter are reduced because of the 7X higher switching frequency.

#### C. High Temperature Capability of the SiC Converter

The SiC converter has high efficiency (98.5 % – 99.0 % at

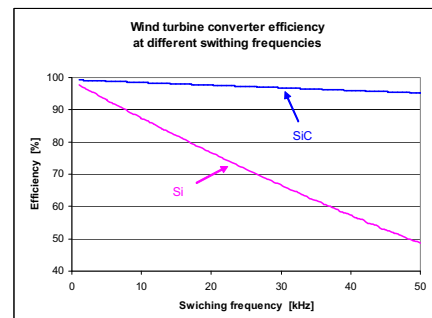


Fig. 9. Efficiency of SiC and Si wind turbine converters at different switching frequencies.

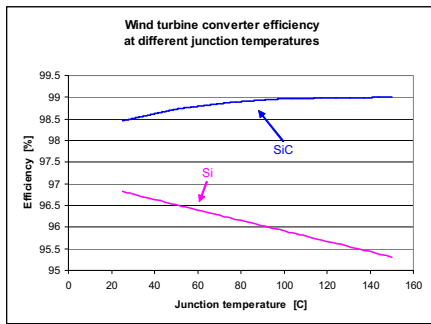


Fig. 10. Power loss breakdown in the wind generation system.

3 kHz and rated power) at the temperature range from 25 °C to 150 °C. While the efficiency of the Si converter is lowered by 1.5 % from 25 °C to 150 °C (see Fig. 10).

The cooling requirement of the SiC converter can be less than that of the Si converter even with the same temperature limit. As calculated by the simulation, the thermal resistance of the heatsinks required by the SiC converter is 0.152 K/W for the generator rectifier and 0.181 K/W for the grid inverter (assuming these two are on different heatsinks). The values can be realized by a natural convection heatsink, for example, the heatsink E 1357 from Comair Rotron, Inc. [11], and the approximate volume is 3228 cm<sup>3</sup>. The thermal resistance of the heatsinks required by the Si converter is 0.0024 K/W and 0.0062 K/W. Liquid cooling is needed to achieve the values. If Hi-Contact liquid cold plates from Aavid Thermalloy, LLC [12] are used, the volume of the heatsinks will be about 2884 cm<sup>3</sup> (not including any accessories). The volume of the heatsinks of the two systems is close, but that of the SiC converter is much simpler. Furthermore, SiC devices are allowed to work at higher temperature (at least 300 °C) with proper packaging. This can further reduce the size of heatsinks. Therefore, the application of the SiC converter can simplify the thermal management, and save space and expense.

#### IV. CONCLUSIONS

The simulations in this work leads to a conclusion that the application of the SiC converter in the wind generation system will improve the system efficiency, conserve energy, and reduce system size and cost due to the low-loss, high-

frequency, and high-temperature properties of SiC devices even for one-for-one replacement. More benefits can be obtained by elevating the rated voltage of the system in order to take the advantage of the high voltage capability of SiC devices. For any of these benefits to appear in wind generation system, however, will require that manufacturers of SiC switching devices are able to produce sufficient quantities at costs that can show an overall system cost savings in installed cost and/or operating costs of the wind turbines.

#### REFERENCES

- [1] G. Bywaters, V. John, J. Lynch, P. Mattila, G. Norton, J. Stowell, M. Salata, O. Labath, A. Chertok, D. Hablanian, "Northern power systems WindPACT drive train," *Subcontractor Report*, NREL/SR-500-35524, <http://www.nrel.gov/wind/pdfs/35524.pdf>, Apr. 2001- Jan. 2005.
- [2] D. A. Marckx, "Breakthrough in power electronics from SiC," *Subcontractor Report*, NREL/SR-500-38515, <http://www.nrel.gov/wind/pdfs/38515.pdf>, May. 2004- May. 2005.
- [3] J. S. Lai, R. W. Young, G. W. Ott, Jr., J. W. McKeever, "Efficiency modeling and evaluation of a resonant snubber based soft-switching inverter for motor drive applications," *IEEE Power Electronics Specialists Conference*, June 18-22, 1995, pp. 943-949.
- [4] M. H. Bierhoff, F. W. Fuchs, "Semiconductor losses in voltage source and current source IGBT converters based on analytical derivation," *IEEE Power Electronics Specialists Conference*, 2004, pp. 2836-2842.
- [5] F. Blaabjerg, U. Jaeger, S. Munk-Nielsen, "Power losses in PWM-VSI inverter using NPT or PT IGBT devices," *IEEE Transactions on Power Electronics*, vol. 10, no. 3, May 1995, pp. 358-367.
- [6] B. Ozpineci, L. M. Tolbert, S. K. Islam, M. Hasanuzzaman, "Effects of silicon carbide (SiC) power devices on PWM inverter losses," *Annual Conference of the IEEE Industrial Electronics Society*, 2002, Denver, Colorado, pp. 1061-1066.
- [7] H. Zhang, "Electro-thermal modeling of SiC power electronic systems," Ph.D. Dissertation, The University of Tennessee, 2007.
- [8] H. Zhang, L. M. Tolbert, B. Ozpineci, M. Chinthavali, "A SiC-based converter as a utility interface for a battery system," *IEEE Industry Applications Society Annual Meeting*, October 8-12, 2006, Tampa, Florida, pp. 346-350.
- [9] Datasheet of silicon carbide Schottky diode-C2D10120, [www.cree.com/products/pdf/C2D10120.pdf](http://www.cree.com/products/pdf/C2D10120.pdf).
- [10] Datasheet of silicon IGBT module – DIM200WHS17, [www.dynexsemi.com/assets/IGBT\\_Modules/Datasheets/DNX\\_DIM200WHS17-A000.pdf](http://www.dynexsemi.com/assets/IGBT_Modules/Datasheets/DNX_DIM200WHS17-A000.pdf).
- [11] Manufacturer page of E1357 from Comair Rotron, Inc., [www.thermaflo.com/bin/cr\\_exdatasht.pl?Pnum=e1357&ExLength=3&LengthUnits=in&SearchButton1=Change+Length](http://www.thermaflo.com/bin/cr_exdatasht.pl?Pnum=e1357&ExLength=3&LengthUnits=in&SearchButton1=Change+Length).
- [12] Manufacturer page of Hi-Contact liquid cold plates from Aavid Thermalloy, LLC, [www.aavidthermalloy.com/products/liquid/hi-contact.pdf](http://www.aavidthermalloy.com/products/liquid/hi-contact.pdf).